

EXPRESS LETTER

Excess strain in the Echigo Plain sedimentary basin, NE Japan: evidence from coseismic deformation of the 2011 Tohoku-oki earthquake

T. Nishimura,¹ H. Suito,² T. Kobayashi,² Q. Dong³ and T. Shibayama⁴

¹Disaster Prevention Research Institute, Kyoto University, Gokasho, Uji, Kyoto Prefecture 611-0011, Japan. E-mail: nishimura.takuya.4s@kyoto-u.ac.jp

²Geography and Crustal Dynamics Research Center, Geospatial Information Authority of Japan, Kitasato 1, Tsukuba, Ibaraki Prefecture 305-0081, Japan

³EduScience Research Institute Corporation, Higashimita 3-10-1-524, Tama-ku, Kawasaki, Kanagawa Prefecture 214-0033, Japan

⁴Research Center of Computational Mechanics Inc., Togoshi NI building, Togoshi 1-7-1, Shinagawa-ku, Tokyo 142-0041, Japan

Accepted 2016 March 10. Received 2016 March 10; in original form 2015 October 20

SUMMARY

Coseismic deformation depends on both the source fault and on the elastic properties of the crust. Large coseismic deformation associated with the 2011 M_w 9.0 Tohoku-oki earthquake enabled us to investigate strain anomalies from crustal inhomogeneity. Concentrated contractional strain was observed in the Echigo Plain (Niigata-Kobe Tectonic Zone) before the Tohoku-oki earthquake, whereas continuous and campaign global navigation satellite system measurements show a widespread distribution of coseismic extensional strain in and around the plain. A 1-D displacement profile shows high strain (7.2 ± 0.7 microstrain) in a 17 km long section across the Echigo Plain and low strain (3.3 ± 0.4 microstrain) along a 15 km long section east of the plain, despite the latter being closer to the megathrust fault source. We performed numerical modelling of coseismic deformation using a heterogeneous subsurface structure and successfully reproduced excess extension in the plain, which is filled by low-rigidity sediments. This study demonstrates the importance of considering heterogeneous crust in deformation modelling.

Key words: Satellite geodesy; Kinematics of crustal and mantle deformation; High strain deformation zones; Asia.

1 INTRODUCTION

Elastic heterogeneity of the crust causes strain anomalies and displacement distributions that deviate from those predicted by uniform elastic half-space models (e.g. Pollitz *et al.* 2008; Segall 2010). However, identifying the source of observed strain anomalies such as elastic heterogeneity, measurement uncertainties or locally triggered deformation remains a challenge in practice because these sources cause similar surface deformation anomalies. The M_w 9.0 Tohoku-oki earthquake occurred on 2011 March 11 caused large-scale crustal deformation in and around the Japanese archipelago (Ozawa *et al.* 2012). The detailed distribution of the coseismic deformation was observed by a dense, continuous global navigation satellite system (GNSS) network and Synthetic Aperture Radar (SAR) interferometry (e.g. Kobayashi *et al.* 2011; Nishimura *et al.* 2011). These data provided an ideal opportunity to investigate locally anomalous deformation that deviates from the simple elastic response predicted by dislocation models embedded in a homogeneous half-space (e.g. Okada 1992).

For instance, Ohzono *et al.* (2012) investigated local deformation anomalies using GNSS Earth Observation Network System

(GEONET) data and found relatively small and large extensions which were possibly caused by elastic heterogeneity in the Ou-backbone Range and the Niigata-Kobe Tectonic Zone (NKTZ) of northeastern Japan, respectively.

The NKTZ (Fig. 1) is a strain concentration zone in the back-arc region of northeastern Japan that has been identified by geodetic measurements, geomorphologic studies and high seismicity (Sagiya *et al.* 2000). Geodetic measurements showed a high rate of contractional oriented WNW–ESE strain in the region for a century before the Tohoku-oki earthquake. The width of the strain concentration zone is roughly 100 km, varying along strike. Based on GNSS data between April 1998 and February 2011 and triangulation/trilateration data between 1899 and 1991, Nishimura *et al.* (2012) found that contractional deformation is concentrated in a ~25 km wide zone corresponding to the Echigo Plain, which is located at the mouth of two large rivers that discharge into the Sea of Japan. The Echigo Plain is a sedimentary plain containing a deep extensional rift that formed between 13 and 16 Ma and is filled by Miocene and younger sediments (e.g. Okada & Ikeda 2012). However, the tectonic stress regime changed to compression at 3.5 Ma. Recent earthquakes near the plain have included the 2004

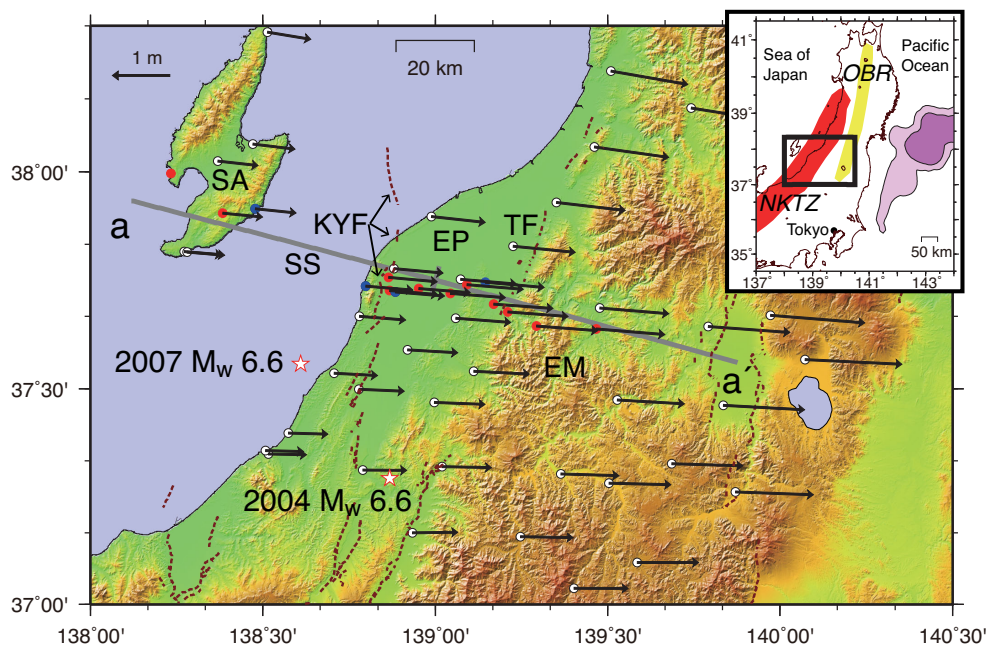


Figure 1. Displacement from 2010 to 2011, including coseismic displacement associated with the 2011 Tohoku-oki earthquake, observed at global navigation satellite system (GNSS) stations. Blue and red circles denote continuous and campaign GNSS stations, respectively, white circles denote continuous GNSS Earth Observation Network System (GEONET) stations and brown lines denote surface traces of active faults (Earthquake Research Committee, <http://www.jishin.go.jp/main/index-e.html>, last accessed 14 March 2016). SA, SS, EP, EM, KYF and TF denote the Sado, Sado Straight, Echigo Plain, Echigo Mountains, Kakuda-Yahiko fault and Tsukioka fault, respectively. The inset regional map shows the location of the study area enclosed in the black rectangle. The red and yellow shaded regions denote the Niigata-Kobe Tectonic Zone (NKTZ) and the Ou Backbone Range (OBR). Pale and bright pink regions represent the coseismic slip areas of the Tohoku-oki earthquake with ≥ 5 and ≥ 20 m slips, respectively (Ozawa *et al.* 2012).

M_w 6.6 mid-Niigata prefecture event and the 2007 M_w 6.6 Niigataken Chuetsu-oki event (Kato *et al.* 2006). The compressional axis of their focal mechanisms were directed WNW–ESE, which is concordant with the geodetic strain. Active folds and faults (i.e. the Kakuda-Yahiko fault, the Tsukioka fault and the Niitsu anticline) exist at both the eastern and western rims of the plain (Figs 1 and 2; i.e. Okada & Ikeda 2012). These features suggest that long-term contractional deformation is concentrated near the rims of the plain, rather than in the interior.

In order to identify the detailed distribution and partitioning of contractional deformation and to understand deformation mechanisms and earthquake potential, we collected GNSS observations at 4 continuous and 10 campaign stations oriented N120°E along the principle axis of the contractional strain across the Echigo Plain in 2010. However, achieving our original objective was challenging because the relevant data were masked by large coseismic and post-seismic deformation associated with the Tohoku-oki earthquake. Instead, our GNSS array allowed us to investigate the detailed spatial pattern of the 2011 Tohoku-oki earthquake coseismic deformation. We then performed Finite Element Method (FEM) modelling to demonstrate how strain anomalies are produced by weak sediments in the Echigo Plain. Finally, we considered the implications for regional deformation mechanisms.

2 GNSS DATA AND ANALYSIS

The data used in this study were acquired at continuous GNSS GEONET stations and at our own continuous and campaign stations (Fig. 1). We used Trimble 5700 receivers and Zephyr geodetic (or Zephyr 2 geodetic) antenna, with the GNSS antenna fixed to the roofs of concrete buildings with steel bolts. An annual GNSS campaign has been conducted simultaneously for all stations every fall since 2010. Although the stations are generally occupied by

GNSS equipment for at least 4 weeks in each campaign, for two stations the 2010 campaign data are only available for a few days because of power failures. Daily coordinates for all GNSS stations were estimated by precise point positioning with ambiguity resolution (Bertiger *et al.* 2010) using the GIPSY-OASIS ver. 6.2 software. Daily coordinates were transformed into the IGB08 reference frame (<https://igscb.jpl.nasa.gov/network/refframe.html>, last accessed 14 March 2016) using transformation parameters provided by the Jet Propulsion Laboratory. We calculated the means of the daily coordinates for 1 October to 20 November in 2010 and 2011. Except for the two problematic stations, standard deviations in the 2010 measurements were 1.2–2.8, 1.6–3.3 and 7.8–13.3 mm for the north, east and vertical components of the position, respectively, while those in the 2011 measurements were 1.7–3.5, 2.5–11.9 and 4.1–10.6 mm, respectively. The larger standard deviations in the east component of the 2011 data reflect post-seismic deformation following the 2011 Tohoku-oki earthquake. As of October 2011, post-seismic deformation occurred at a rate of ~ 25 mm month⁻¹ at the most rapid stations. By subtracting the 2010 means from the 2011 means, we calculated the displacement from 2010 to 2011 (Fig. 1). The observed displacement was mainly caused by the 2011 Tohoku-oki earthquake and was characterized by an increase in eastward displacement toward the northeast. Uncertainties in the horizontal displacement (with a 99.7 per cent confidence limit) ranged between 6.9 and 41 mm. We did not consider vertical displacement in this study because of its large measurement uncertainties and possible unknown offsets due to the reinstallation of GNSS antennas for the campaign sites.

We rotated the horizontal displacement along profile a–a', which was oriented N105°E, roughly parallel to our GNSS array. The displacement in the N105°E and N15°E directions were plotted for stations within 10 km of the profile (Fig. 2). Displacement was similar at adjacent stations, which allowed us to eliminate large local deformation and instability of the GNSS monument.

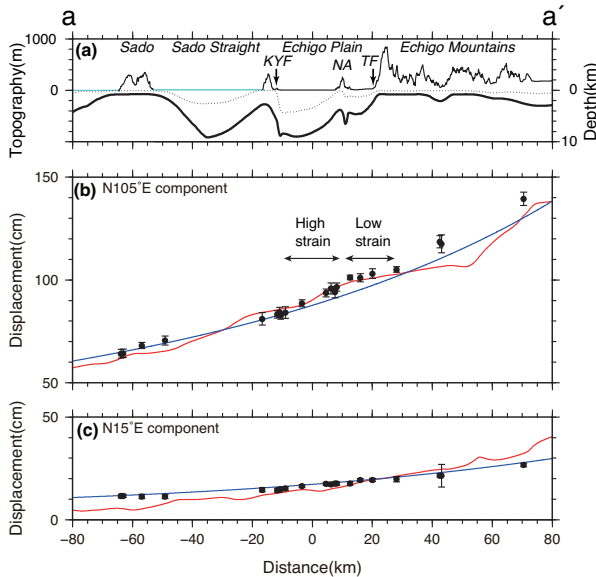


Figure 2. Displacement along profile a–a' (Fig. 1) from 2010 to 2011. (a) Topography and subsurface structure along the profile. Thin, dotted and thick lines show the elevation of topography and the depths for layers with $V_s = 1.7$ and 2.7 km s^{-1} in the J-SHIS structure model (Fujiwara *et al.* 2008), respectively. Sky blue topography represents sea level. KYF, NA and TF denote the Kakuda-Yahiko fault, Niitsu anticline and Tsukioka fault, respectively. (b) Displacement components parallel to the profile (i.e. N105°E). Black circles represent the displacement observed at GNSS stations within 10 km of the profile between 2010 and 2011. Error bars represent 3σ . Blue and red curves are 1.28 times coseismic displacement of the Tohoku-oki earthquake predicted using homogeneous and heterogeneous structure models, respectively (see the text). Arbitrary offsets for calculated displacement are added to compare a spatial pattern of relative calculated displacement with that of the observed displacement. (c) Displacement perpendicular to the profile.

Displacement in the direction of N105°E increased with increasing distance toward the east; although, its gradient showed spatial variation. The gradient of the observed displacement was steep between -9 and 8 km (hereafter, the western section) and gentle between 13 and 28 km (hereafter, the eastern section). Relative displacement was 12.4 ± 1.2 and $3.9 \pm 0.6 \text{ cm}$ for the western and the eastern sections, respectively, corresponding to 7.2 ± 0.7 and 3.3 ± 0.4 microstrain of extensional strain, respectively. The western section, which corresponded to the main part of the Echigo Plain (between the Kakuda-Yahiko fault and the Niitsu Anticline; Fig. 2) saw extension of more than twice that of the eastern section (near the eastern rim of the Echigo Plain and the Echigo Mountains). Compared to a longer section between -16 and 43 km along the profile (Fig. 2b), which had a mean strain of 6.4 ± 0.3 microstrain and included both subsections, the western and the eastern sections extended excessively and deficiently, respectively.

The observed displacement between 2010 and 2011 included not only coseismic displacement associated with the Tohoku-oki earthquake and aftershocks, but also pre-seismic and post-seismic deformation. We compared the horizontal displacement from 2010 to 2011 with the pure coseismic displacement at continuous sites using the daily coordinates from just before and after the Tohoku-oki earthquakes and found that they were similar but with different amplitudes (Supporting Information Fig. S1). By fitting a linear function between the along-profile displacements, we calculated that year-long displacement was 1.28 ± 0.02 times the coseismic displacement (Supporting Information Fig. S2). This suggests that the observed year-long displacement was proportional to the instan-

taneous elastic response caused by coseismic faulting. We therefore used this value to compare the year-long displacement with the calculated value from elastic deformation modelling. In other words, we always multiply the calculated displacements by 1.28.

3 DEFORMATION MODELLING WITH HOMOGENEOUS AND HETEROGENEOUS STRUCTURES

We first calculated displacement using a homogeneous elastic half-space (e.g. Okada 1992) and the fault model of the 2011 Tohoku-oki earthquake and its largest aftershock (Nishimura *et al.* 2011). The homogeneous elastic response of the Tohoku-oki earthquake resulted in a gradually increasing gradient of the coseismic displacements toward the east (Fig. 2). The source megathrust faults of the Tohoku-oki earthquake are located $\sim 150 \text{ km}$ to the east of the profile; therefore, variations in the fault models did not significantly affect strain distribution along the profile described here (e.g. Ohzono *et al.* 2012). The predicted extensions were 4.4 and 5.3 microstrain in the western and the eastern sections, respectively; however, it was clear that the gradient of the observed displacement was steeper and gentler than that calculated for the western and eastern sections, respectively (Fig. 2). Therefore, we attributed the distribution of the observed strain around the Echigo Plain to a strain anomaly.

Next, we considered the observed strain anomaly resulting from the contrasting elastic properties of the weak sedimentary plain and the eastern hard bedrock mountains. We performed 3-D FEM analyses incorporating a heterogeneous subsurface structure in order to reproduce the observed coseismic strain anomaly. The modelled region consisted of two parts: a coarse-mesh area ranging from 137.5°E to 145.5°E and 35°N to 42°N , and a fine-mesh area ranging from 138°E to 140°E and 37°N to 38.5°N (Supporting Information Fig. S3). The sizes of these parts were $720 \times 770 \times 150$ and $180 \times 165 \times 40 \text{ km}^3$, respectively, in the east, north and vertical directions. The coarse and fine mesh parts were subdivided in hexahedrons with sides of ~ 5 and $\sim 1 \text{ km}$ long, respectively. The total number of hexahedrons was ~ 7.35 million. The fault models of the 2011 Tohoku-oki earthquake (Nishimura *et al.* 2011) were the same used in the modelling with a homogeneous half-space. The elastic properties and densities of each element were assigned by approximating the Japan Seismic Hazard Information Station (J-SHIS) deep subsurface structure model (Fujiwara *et al.* 2008). The Echigo Plain is characterized by extremely thick sedimentary layers (Fig. 2a; Supporting Information Fig. S4a). The depth of the seismic basement layer, which has a P -wave velocity of $\geq 5.0 \text{ km s}^{-1}$, an S -wave velocity of $\geq 2.7 \text{ km s}^{-1}$ and a density of 2500 kg m^{-3} , exceeds 8 km . We did not consider the effects of gravity or the Earth's curvature, which were negligible for the spontaneous elastic response because the GNSS stations extended across a width of 160 km . We calculated elastic displacement using the EduS/FrontISTR FEM code, which is a new scientific research environment for the simulation of crustal movement using the parallel platform of FrontISTR.

The calculated normal strain in the east direction (e_{ee}) showed heterogeneous distribution in the backarc region far from the megathrust source fault (Supporting Information Fig. S4b). The calculated strain in the backarc region was highly dependent on the depth of the seismic basement and rigidity near the surface. The calculated displacement generally explained the observed displacement along the profile (Fig. 2). In particular, the high strain in the Echigo Plain and the low strain along the western rim of the Echigo Mountains were well reproduced by the model. Extensional strain in the western and eastern sections was calculated to be 6.0

and 2.5 microstrain, respectively. Although the calculated strain was a little smaller than the observed strain, the strain ratios for the two sections were approximately equal. However, the observed displacement differed significantly from the calculated displacement at a distance of 43 km (Fig. 2b). This may reflect a problem with the subsurface structure used.

4 DISCUSSION

The observed displacement between 2010 and 2011 included pre-seismic and post-seismic deformation as well as coseismic displacement of the Tohoku-oki earthquake. Before the Tohoku-oki earthquake, slow contractional deformation of less than 1 cm yr^{-1} was observed (Supporting Information Fig. S5a). The observed contractional strain was concentrated in the western section and could be used to reduce the anomalous extension from 2010 to 2011, despite being much smaller than the strain observed from 2010 to 2011. Therefore, we concluded that pre-seismic deformation made a negligible contribution to the strain anomaly in our data set. Extension along the profile has continued in the years after the Tohoku-oki earthquake, albeit at a decreasing rate (Supporting Information Fig. S5b). Post-seismic deformation at continuous stations from 12 March to October and November 2011 clearly showed excess strain in the western section (Supporting Information Fig. S5b). While it is difficult to recognize excess strain in later post-seismic periods (because of the small signal amplitude), the post-seismic strain anomaly was similar to the coseismic strain anomaly. The displacement observed over the year was identical to 1.28 times pure coseismic displacement (Supporting Information Fig. S5c), except for that at a station with a distance of 13 km. The time series of daily coordinates for this exceptional station contains a large nonlinear (mostly seasonal) component, suggesting that this station may have been disturbed by local artificial deformation caused by the pumping of ground water. However, even when this station was excluded from the analysis, the continuous GNSS data confirmed that high strain in the Echigo Plain took place coseismically and continued in the post-seismic period, at least for the first 7 months following the earthquake. We concluded that the low rigidity material in the Echigo Plain resulted in an elastic strain anomaly during both the coseismic and post-seismic periods.

Dense and precise geodetic measurements and large-scale deformation associated with the 2011 Tohoku-oki earthquake have enabled several studies to capture local anomalous deformation caused by elastic and inelastic responses of the heterogeneous crust. Ohzono *et al.* (2012) suggested that excess strain in the NKTZ is caused by a low elastic modulus of the thick sedimentary layer. Our study, which was performed using a dense GNSS array, has identified the detailed spatial distribution of the excess and deficient strain. The highly extensional region corresponded to the main part of the Echigo Plain. By using numerical modelling with a heterogeneous subsurface structure, we obtained results that are consistent with their inferences on the cause of the excess strain.

Following several earthquakes elsewhere in the world, local anomalous deformation signals have been observed in neighbouring fault zones by InSAR measurements (e.g. Wright *et al.* 2001; Fialko *et al.* 2002; Hamiel & Fialko 2007). These signals were explained by triggered slip on faults or by the elastic response of low-rigidity material in fault zones with a width of a few kilometres; nevertheless, it is difficult to distinguish these effects from each other solely based on observed deformation. Owing to the episodic growth of a fault-related fold that was triggered by the 2007 Niigataken Chuetsu-oki earthquake, whose epicentre was just ~ 30 km south of GNSS profile a–a' (Nishimura *et al.* 2008), aseismic slip remains a pos-

sible alternative mechanism to explain the strain anomaly in the Echigo Plain. Deep (i.e. ~ 10 km) slip is required to explain the observed strain anomaly with a spatial scale of more than 10 km. Normal-type slip beneath the Echigo Plain provides the most feasible fit for the excess extensional strain. However, the stress tensor inversion using the earthquake focal mechanism (Yoshida *et al.* 2012) and pre-seismic strain data (Nishimura *et al.* 2012) suggests a compressional stress regime where the principal compressional axis was oriented parallel to profile a–a'. All of the active faults around the Echigo Plain are reverse-type, which are favourable to the compressional stress regime. The 2011 Tohoku-oki earthquake caused large extensional deformation and the change of stress regime from compression to tensile in some Pacific coastal areas close to the megathrust source fault (Yoshida *et al.* 2012). However, the coseismic stress change is small around the Echigo Plain which is far away from the source fault and the compressional stress regime in an absolute sense remained around the Echigo Plain after the Tohoku-oki earthquake (Yoshida *et al.* 2012); therefore, it is not plausible that aseismic slip occurred.

It is interesting that deformation in the Echigo Plain was larger than that in the surrounding regions, not only during the coseismic period but also during the pre-seismic period; although, the deformation modes (i.e. extension or contraction) of the two periods were opposite (Supporting Information Fig. S5). Nishimura *et al.* (2012) proposed that elastic strain due to interplate coupling on the subducting Pacific Plate is not the main cause of the strain concentration in the Echigo Plain because the contractional strain rate remained almost constant (~ 0.2 microstrain yr^{-1}) over the 15 years before the 2011 Tohoku-oki earthquake; although, that in the nearby forearc region was strongly affected by interplate coupling and changed with time considerably. They also suggested that strain concentration during the pre-seismic period could be attributed to steady creep on down-dip parts of reverse faults along the eastern and western rims of the Echigo Plain. The results of this study suggest that a low elastic modulus of the sedimentary plain must have somewhat contributed to the concentration of contractional strain before 2011. Further analysis of the observed pre-seismic, coseismic and post-seismic deformation is needed in order to constrain the mechanism of strain concentration in the Echigo Plain of the NKTZ.

Using the dislocation model in a homogeneous elastic half-space is a standard approach for modelling seismic and volcanic deformation. However, previous studies have suggested that a heterogeneous subsurface structure provides a significant impact on surface displacement at both the large scale (e.g. plate boundary zones; Schmalzle *et al.* 2006; Sato *et al.* 2007) and the small scale (e.g. fault zones; Fialko *et al.* 2002; Hamiel & Fialko 2007). The results of this study have shown a strain anomaly at an intermediate scale (tens of kilometres). Geodetic data in sedimentary plains and basins with thick sediments require special attention as they may bias estimations of source magnitudes. In such cases, numerical modelling using heterogeneous elastic properties become important for fitting high-accuracy dense geodetic data acquired by GNSS and InSAR, or other techniques and data sets to measure surface deformation over time.

5 CONCLUSIONS

We examined the detailed spatial pattern of coseismic deformation associated with the 2011 M_w 9.0 Tohoku-oki earthquake in the Echigo Plain, NKTZ, using geodetic data acquired from a dense GNSS array and GEONET stations. Deformation from October 2010 to October 2011 showed 7.2 and 3.3 microstrain of extensional strain along western (a 17 km long section across the plain)

and eastern (a 15 km long section near the eastern rim of the plain) profiles, respectively. These strain variations contradicted those of the elastic deformation predicted by a dislocation model in a homogeneous half-space because the eastern section was closer to the source fault of the Tohoku-oki earthquake. In the section of excess strain, the contractional strain rate had been concentrated before the 2011 Tohoku-oki earthquake. A numerical calculation using FEM with a subsurface structure based on seismic velocity models (Fujiwara *et al.* 2008) suggested that the observed coseismic strain anomaly was caused by weak sedimentary material with a low elastic-modulus. While the observed strain concentration before 2011 has been modelled by creep on down-dip extensions of active faults along the eastern and western rims of the Echigo Plain (Nishimura *et al.* 2012), we propose that weak sediments may have contributed significantly to the strain concentration. The results of this study suggest that elastic heterogeneity of the subsurface structure substantially affects the modelling of seismic deformation observed using precise geodetic techniques.

ACKNOWLEDGEMENTS

The GNSS data used in this study can be obtained from the corresponding author via e-mail. Constructive comments by Roland Bürgmann, Felipe Aron and Editor Jörg Renner improved the quality of the paper. This study was supported by a special research project of the Geospatial Information Authority of Japan (GSI) and the Japan Society of the Promotion of Science (JSPS) Grants-in Aid for Scientific Research (KAKENHI; Grant Number 26109007). FrontISTR is an open source software developed by the project 'Research and Development for Innovative Simulation Software' at the Center for Research on Innovative Simulation Software (CISS), The University of Tokyo.

REFERENCES

- Bertiger, W., Desai, S., Haines, B., Harvey, N., Moore, A.W., Owen, S. & Weiss, J.P., 2010. Single receiver phase ambiguity resolution with GPS data, *J. Geod.*, **84**, 327–337.
- Fialko, Y., Sandwell, D., Agnew, D., Simons, M., Shearer, P. & Minster, B., 2002. Deformation on nearby faults induced by the 1999 Hector Mine earthquake, *Science*, **297**, 1858–1862.
- Fujiwara, H. *et al.*, 2008. A study on subsurface structure model for deep sedimentary layers of Japan for strong motion evaluation (in Japanese), *Technical Note of the National Research Institute for Earth Science and Disaster Prevention*, No. 337, Tsukuba, Japan.
- Hamiel, Y. & Fialko, Y., 2007. Structure and mechanical properties of faults in the North Anatolian Fault system from InSAR observations of coseismic deformation due to the 1999 Izmit (Turkey) earthquake, *J. geophys. Res.*, **112**, B07412, doi:10.1029/2006JB004777.
- Kato, A., Sakai, S., Hirata, N., Kurashimo, E., Iidaka, T., Iwasaki, T. & Kanazawa, T., 2006. Imaging the seismic structure and stress field in the source region of the 2004 mid-Niigata prefecture earthquake: structural zones of weakness and seismogenic stress concentration by ductile flow, *J. geophys. Res.*, **111**, B08308, doi:10.1029/2005JB004016.
- Kobayashi, T., Tobita, M., Nishimura, T., Suzuki, A., Noguchi, Y. & Yamanaka, M., 2011. Crustal deformation map for the 2011 off the Pacific coast of Tohoku Earthquake, detected by InSAR analysis combined with GEONET data, *Earth Planets Space*, **63**(7), 621–625.
- Nishimura, T., Tobita, M., Yurai, H., Amagai, T., Fujiwara, M., Ue, H. & Koarai, M., 2008. Episodic growth of fault-related fold in northern Japan observed by SAR interferometry, *Geophys. Res. Lett.*, **35**, L13301, doi:10.1029/2008GL034337.
- Nishimura, T., Munekane, H. & Yurai, H., 2011. The 2011 off the Pacific coast of Tohoku Earthquake and its aftershocks observed by GEONET, *Earth Planets Space*, **63**, 631–636.

- Nishimura, T., Suito, H., Kobayashi, T. & Tobita, M., 2012. Crustal deformation in and around the Echigo Plain clarified by geodetic observation across the Niigata-Kobe Tectonic Zone (in Japanese with English abstract), *Zisin, J. Seismol. Soc. Japan*, **64**, 211–222.
- Ohzono, M., Yabe, Y., Inuma, T., Ohta, Y., Miura, S., Tachibana, K., Sato, T. & Demachi, T., 2012. Strain anomalies induced by the 2011 Tohoku Earthquake (M_w 9.0) as observed by a dense GPS network in the north-eastern Japan, *Earth Planets Space*, **64**, 1231–1238.
- Okada, Y., 1992. Internal deformation due to shear and tensile faults in a half-space, *Bull. seism. Soc. Am.*, **82**, 1018–1040.
- Okada, S. & Ikeda, Y., 2012. Quantifying crustal extension and shortening in the back-arc region of Northeast Japan, *J. geophys. Res.*, **117**, B01404, doi:10.1029/2011JB008355.
- Ozawa, S., Nishimura, T., Munekane, H., Suito, H., Kobayashi, T., Tobita, M. & Imakiire, T., 2012. Preceding, coseismic, and postseismic slips of the 2011 Tohoku earthquake, Japan, *J. geophys. Res.*, **117**, B07404, doi:10.1029/2011JB009120.
- Pollitz, F.F., McCrory, P., Svarc, J. & Murray, J., 2008. Dislocation models of interseismic deformation in the western United States, *J. geophys. Res.*, **113**, B04413, doi:10.1029/2007JB005174.
- Sagiya, T., Miyazaki, S. & Tada, T., 2000. Continuous GPS array and present-day crustal deformation of Japan, *Pure appl. geophys.*, **157**(11), 2303–2322.
- Sato, K., Minagawa, N., Hyodo, M., Baba, T., Hori, T. & Kaneda, Y., 2007. Effect of elastic inhomogeneity on the surface displacements in the north-eastern Japan: based on three-dimensional numerical modeling, *Earth Planets Space*, **59**, 1083–1093.
- Schmalzle, G., Dixon, T., Malservisi, R. & Govers, R., 2006. Strain accumulation across the Carrizo segment of the San Andreas Fault, California: impact of laterally varying crustal properties, *J. geophys. Res.*, **111**, B05403, doi:10.1029/2005JB003843.
- Segall, P., 2010. *Earthquake and Volcano Deformation*, pp. 118–165, Princeton Univ. Press.
- Wright, T., Fielding, E. & Parsons, B., 2001. Triggered slip: observations of the 17 August 1999 Izmit (Turkey) earthquake using radar interferometry, *Geophys. Res. Lett.*, **28**, 1079–1082.
- Yoshida, K., Hasegawa, A., Okada, T., Inuma, T., Ito, Y. & Asano, Y., 2012. Stress before and after the 2011 great Tohoku-oki earthquake and induced earthquakes in inland areas of eastern Japan, *Geophys. Res. Lett.*, **39**, L03302, doi:10.1029/2011GL049729.

SUPPORTING INFORMATION

Additional Supporting Information may be found in the online version of this paper:

Figure S1. Comparison between yearly and 2 d long horizontal displacements including the 2011 Tohoku-oki earthquake at continuous GNSS stations.

Figure S2. Comparison between yearly and 2 d long N105°E displacements including the 2011 Tohoku-oki earthquake at continuous GNSS stations along profile a–a'.

Figure S3. Configuration of the Finite Element Method (FEM) mesh for the deformation modelling.

Figure S4. Distribution of the depth of the seismic bedrock and strain calculated using the Finite Element Method (FEM).

Figure S5. Deformation along the profile a–a' before and after the 2011 Tohoku-oki earthquake. All displacements and velocities represent along-profile (i.e., N105°E) components. Error bars represent three sigma (<http://gji.oxfordjournals.org/lookup/suppl/doi:10.1093/gji/ggw102/-/DC1>).

Please note: Oxford University Press is not responsible for the content or functionality of any supporting materials supplied by the authors. Any queries (other than missing material) should be directed to the corresponding author for the paper.